S-layer of *Lactobacillus helveticus* MIMLh5 promotes endocytosis by dendritic cells

Running title: MIMLh5's S-layer drives endocytosis in DCs

Valentina Taverniti[a#], Mauro Marengo[a], Eva Fuglsang[b], Helene Marie Skovsted[b], Stefania Arioli[a], Giacomo Mantegazza[a], Giorgio Gargari[a], Stefania Iametti[a], Francesco Bonomi[a], Simone Guglielmetti[a] and Hanne Frøkiær[b#]

[a] Department of Food, Environmental and Nutritional Sciences, Università degli Studi di Milano, Italy

[b] Department of Veterinary and Animal Sciences, University of Copenhagen, 1870 Frederiksberg, Denmark

#Corresponding authors: hafr@sund.ku.dk & valentina.taverniti@unimi.it

ABSTRACT

S-layers are proteinaceous arrays covering the cell wall of numerous bacteria. Their suggested properties, like the interaction with host immune system, have been only poorly described. Here, we aimed at elucidating the role of S-layer from the probiotic bacterial strain *Lactobacillus helveticus* MIMLh5 in the stimulation of murine bone marrow-derived dendritic cells (DCs). MIMLh5 induced a higher production of IFN-β, IL-12 and IL-10 compared to S-layer-depleted MIMLh5 (n-MIMLh5), whereas the isolated S-layer was a poor immunostimulator. No difference was found in the production of TNF-α and IL-1β. Inhibition of the MAP kinases JNK1/2, p38 and ERK1/2 modified IL-12 production similarly in MIMLh5 and n-MIMLh5, suggesting the induction of the same signaling pathways by the two bacterial preparations. Treatment of DCs with cytochalasin D to inhibit endocytosis before addition of fluorescence-labeled MIMLh5 cells led to a dramatic reduction in the proportion of fluorescence-positive DCs, and to decreased IL-12 production. Endocytosis and IL-12 production were only marginally affected by cytochalasin D pre-treatment when using fluorescent n-MIMLh5. Treating DCs with S-layer-coated fluorescence-labeled polystyrene beads (Sl-beads) resulted in a much higher uptake of beads compared to non-coated beads. Pre-stimulation of DCs with cytochalasin D reduced the uptake of Sl-beads more than plain beads. These findings indicate that S-layer plays a role in the endocytosis of MIMLh5 by DCs. In conclusion, this study provides evidence that the S-layer of *L. helveticus* MIMLh5 is involved in endocytosis of the bacterium, which is of importance for a strong Th1 inducing cytokine production.

IMPORTANCE

Beneficial microbes may positively impact on host's physiology at various levels, *e.g.* by participating in immune system maturation and modulation, boosting defenses and dampening reactions, therefore affecting the whole homeostasis. As a consequence, the use of probiotics is increasingly regarded as suitable for a more extended application for health maintenance, not only

restricted to microbiotas balancing. Evidently, this implies a deep knowledge of the mechanisms and molecules involved in host-microbes interaction, to the final purpose to fine-tune the choice of a probiotic strain for a specific outcome. To this aim, studies targeted to the description of strain-related immunomodulatory effects and individuation of bacterial molecules responsible for specific responses are indispensable. In this perspective, this study provides a new insight in the characterization of the food-origin probiotic bacterium *L. helveticus* MIMLh5 and its S-layer protein as driver for the cross-talk with dendritic cells.

Keywords: probiotic, nanoparticles, MAPKs, cytokines, cytochalasin D

INTRODUCTION

Surface (S)-layers are bi-dimensional crystalline arrays of proteins, which form an outer self-assembled envelope on the bacterial cell wall. S-layer proteins are ubiquitously present in Archea, Gram-positive and Gram-negative bacteria (Fagan & Fairweather, 2014). They are composed of numerous identical subunits forming a symmetrical, porous, lattice-like layer that completely covers the cell surface. Considering the metabolic efforts that S-layer biogenesis, translocation and assembly imply for bacterial cell, these proteins are expected to play important functions for the organism. Several studies have evidenced different functions connected to the presence of S-layer proteins on bacterial surface, such as virulence, adhesion, protection, degradative activities (*e.g.*, amidase), and molecular sieving (Zhu et al., 2017). Within beneficial bacteria, several *Lactobacillus* species are equipped with S-layer proteins, including *L. helveticus*. In comparison with other bacteria, *Lactobacillus* S-layer proteins are characterized by their small size and high p*I* (Hynönen & Palva, 2013). Mostly, S-layers of lactobacilli have been shown to hold adhesive (Sun et al., 2012; de Leeuw et al., 2006) and immunomodulatory properties (Lightfoot et al., 2015; Taverniti et al., 2013; Li et al., 2011; Konstantinov et al., 2008). However, our understanding of S-layer's role in immune modulation is still limited.

We have previously described *L. helveticus* MIMLh5 as a probiotic strain (Taverniti et al., 2017; Taverniti et al., 2012; Guglielmetti et al., 2010a; Guglielmetti et al., 2010b). We also reported that the isolated S-layer protein induced the expression of TNF-α and COX-2 in the human monocyte-derived cell line U937, and in murine bone marrow-derived and peritoneal cavity-isolated macrophages (Taverniti et al., 2013). In those studies, we observed that depletion of the S-layer from the surface of *L. helveticus* MIMLh5 decreased the ability of the bacterium to induce TNF-α and COX-2, leaving the expression of IL-10 unaltered. In contrast, Konstantinov and collaborators demonstrated a role of the S-layer (SlpA) from *L. acidophilus* NCFM in eliciting the production of the anti-inflammatory cytokine IL-10 in human dendritic cells (DC) *via* interaction with the C-type lectin DC-SIGN receptor, whereas a more pro-inflammatory profile emerged in presence of a *L. acidophilus* NCFM knockout mutant lacking the SlpA (Konstantinov et al., 2008).

Dendritic cells (DCs) use two different strategies dependent on actin polymerization to endocytose bacteria and other particles larger than 800 nm: (i) phagocytosis, an endocytic process that requires the interaction between multiple microbial ligands and DCs receptors (Savina & Amigorena, 2007); and (ii) macropinocytosis, a non-specific uptake of components present in the surrounding fluid (Liu & Roche, 2015). Reportedly, endocytosis of *Lactobacillus acidophilus* NCFM by bone marrow-derived DCs induced IFN-β production, that in turn activated the expression of numerous genes, including IL-12 (Weiss et al., 2010a,b, 2012). In addition, evidence was provided that both phagocytosis and constitutive macropinocytosis contribute to the uptake of strain NCFM (Boye et al., 2016). Lack of stimulation of plasma membrane Toll-Like receptors (TLRs) prior to endocytosis was also shown to be a prerequisite for a strong INF-β/IL-12 induction (Boye et al, 2016) by *L. acidophilus* NCFM, whose S-layer protein shares high similarity with that of *L. helveticus* MIMLh5 (73% identity, 83% positivity; Stuknytė et al., 2014).

Here we investigated the role of MIMLh5 S-layer in the induction of IL-12 production by DCs and its possible role in endocytosis of the bacterium, by comparing the effects of DC stimulation with untreated MIMLh5 and S-layer-depleted MIMLh5 (naked (n)-MIMLh5). We also tested the

purified MIMLh5 S-layer protein, and S-layer-coated polystyrene beads (Sl-beads, ~ 800 nm diameter) to mimic the interaction of the protein with immune cells when the protein is anchored on the surface of particles having size of a bacterium.

MATERIALS AND METHODS

***L. helveticus* MIMLh5 preparation and growth conditions**. *L. helveticus* MIMLh5 was grown in de Man-Rogosa-Sharpe (MRS) broth (Difco Laboratories Inc., Detroit, MI, USA) inoculated from frozen glycerol stocks and sub-cultured twice in MRS using 1:100 inocula. To prepare cultures to be used in immunological experiments, bacteria from an overnight culture were collected, washed twice with sterile PBS, counted with Neubauer counting chamber, resuspended at a concentration of 5×10^9 cells ml^{-1} in PBS, and stored in aliquots at -80 ^{o}C. For preparation of n-MIMLh5, the cell pellet obtained after LiCl treatment (described below) was collected, washed 3 times with PBS to remove residual LiCl, resuspended in PBS, counted and brought to the same cell concentration as MIMLh5, and stored in aliquots at -80°C.

Extraction, purification and chemical characterization of the S-layer protein from *L. helveticus* MIMLh5. Extraction of the S-layer protein from *L. helveticus* MIMLh5 was performed with high-molarity LiCl as described previously (Taverniti et al., 2013; Smit et al., 2001). Briefly, cells from 500 ml of an overnight culture of MIMLh5 were harvested by centrifugation at 10,000 *g* for 20 min at 4 °C and washed with 1 volume of cold sterile MilliQ water. The cell pellet was extracted with 0.1 volume (referred to the starting broth culture volume) of 1 M LiCl for 30 min at room temperature in the presence of a Protease Inhibitor Cocktail (Sigma-Aldrich, Darmstadt, Germany) with slight agitation. After centrifugation, the pellet was extracted with 0.1 volumes of 5 M LiCl for 1 h at room temperature in the presence of Protease Inhibitor Cocktail, and centrifuged. The residual pellet was used to prepare n-MIMLh5 cells (described above), whereas the supernatant was filtered through a 0.2 μm filter and exhaustively dialyzed for 36 h at 4 °C against distilled water containing 0.001% of Protease Inhibitor Cocktail. Dialysis was carried out with 12000 kDa cut-off

membranes (Sigma-Aldrich) that were previously boiled in 2% $NaHCO_3$ and 1 mM EDTA. The dialysate was collected and centrifuged at 20,000 *g* for 20 min at 4 °C. The supernatant was removed, and the pellet was resuspended in sterile MilliQ water and freeze dried. The lyophilized pellet was afterwards resuspended at a concentration of 1 mg ml^{-1} in PBS and stored as aliquots at -80°C. Protein purity was determined by sodium dodecyl sulphate-polyacrylamide gel electrophoresis (SDS–PAGE) and reverse phase (RP)–HPLC/ESI-MS analysis as previously described (Taverniti et al., 2013). *SDS–PAGE*. S-layer protein and total bacterial lysates were resuspended in SDS–PAGE (Laemmli) sample buffer, boiled for 5 min, and separated on 10% polyacrylamide gel in TRIS–glycine–SDS buffer on Mini-PROTEAN 3 system (Bio-Rad). Gels were stained with Coomassie Brilliant Blue G-250 (Sigma–Aldrich, St Louis, MO).

Generation of bone marrow-derived dendritic cells. Bone marrow-derived DCs were prepared as described previously (Christensen et al., 2002). Briefly, bone marrow from C57BL/6 mice (Taconic, Lille Skensved, Denmark) was flushed out from the femur and tibia and washed. 3×10^5 cells ml^{-1} bone marrow cells were seeded into 10 cm Petri dishes in 10 ml RPMI 1640 (Sigma-Aldrich, St. Louis, MO, USA) containing 10% (v/v) heat inactivated fetal calf serum supplemented with penicillin (100 U ml^{-1}), streptomycin (100 mg ml^{-1}), glutamine (4 mM), 50 mM 2-mercaptoethanol (all purchased from Cambrex Bio Whittaker) and 15 ng ml^{-1} murine GM-CSF (harvested from a GM-CSF transfected Ag8.653 myeloma cell line). The cells were incubated for 8 days at 37 °C in 5% CO_2 humidified atmosphere. On day 3, 10 ml of complete medium containing 15 ng/ml GM-CSF was added. On day 6, 10 ml were removed and replaced by fresh medium. Non-adherent, immature DCs were harvested on day 8.

Stimulation of DCs with bacterial cells, bacterial molecules and beads. Immature DCs (2×10^6 cells ml^{-1}) were resuspended in fresh medium supplemented with 10 ng ml^{-1} GM-CSF, and 500 µl $well^{-1}$ of DCs suspension were seeded in 48-well tissue culture plates (Nunc, Roskilde, Denmark). *Lactobacillus helveticus* MIMLh5 was tested at multiplicity of infection (MOI) values of 5 and 50. S-layer protein from *L. helveticus* MIMLh5 was used at 10 µg ml^{-1}. Lipopolysaccharide (LPS) from

Escherichia coli (Sigma-Aldrich) was used in all experiments as internal control at 1 μg ml^{-1} (not shown). Uncoated beads and S-layer-coated beads were used at corresponding MOIs of 5 and 50 for ELISA experiments. Cytochalasin D (Sigma-Aldrich) was added at a concentration of 0.5 μg ml^{-1} 1 h prior to the incubation of DCs with bacteria. In the MAPK inhibition experiments, DCs (2×10^6 cells ml^{-1}) were pre-incubated for 1 h with (i) SP600125 (final concentration 25 μM), a specific inhibitor of JNK1/2 (Invivogen, San Diego, CA, USA), (ii) SB203580 (final concentration 10 μM), a specific inhibitor of p38 MAPK (Invivogen), and (iii) the MEK1/2 inhibitor U0126 (final concentration 10 μM) which blocks MEK1/2 and thereby phosphorylation of the target ERK1/2 (Cell Signaling, MA, USA). In all the conditions described, DCs and stimuli were incubated at 37 °C in 5% CO_2. For time course experiments, DCs were harvested for RNA extraction after 2, 4, 6, and 10 h; the supernatant for ELISA analysis was collected after 4, 6, 10, and 20 h. In the other experiments, DCs were harvested for RNA extraction after 4 or 6 h, and the supernatant for ELISA analysis after 20 h.

Cytokine quantification in DCs supernatant. The concentration of IL-12(p70), IL-10, TNF-α and IL-1β was analyzed by using commercially available ELISA Antibody pairs (R&D systems, Minneapolis, MN, USA) and the concentration of IFN-β by an ELISA kit from PBL Assay Science (Piscataway, NJ, USA) according to the manufacturers' instructions.

RNA extraction. Murine bone marrow-derived DCs were harvested and total RNA was extracted using the MagMAX sample separation system (Applied Biosystems, Foster City, CA, USA), including a DNAse treatment step for genomic DNA removal. RNA concentration was determined by Nanodrop (Thermo, Wilmington, DE, USA).

Reverse transcription and qPCR reaction (RT-qPCR). Five hundred nanograms of total RNA was reverse-transcripted by the TaqMan Reverse Transcription Reagent kit (Applied Biosystems, Foster City, CA, USA) using random hexamer primers according to the manufacturer's instructions. The obtained cDNA was stored in aliquots at -80 °C. Primers and probes were obtained and sequenced as described previously (Boye et al., 2016; Weiss et al., 2013, 2011). qPCR amplifications were carried out in a total volume of 10 μl containing 1×TaqMan Universal PCR Master Mix (Applied Biosystems),

forward and reverse primers, TaqMan MGB probe, and the purified target cDNA (6 ng). Cycling was initiated for 20 s at 95 °C, followed by 40 cycles of 3 s at 95 °C and 30 s at 60 °C using an ABI Prism 7500 (Applied Biosystems). Amplification reactions were performed in triplicate, and DNA contamination controls were included. The amplifications were normalized to the expression of the beta-actin encoding gene. Relative transcript levels were calculated applying the $2^{(-\Delta\Delta C(T))}$ method (Livak & Schmittgen, 2001).

Preparation of fluorescence-labelled bacteria. For endocytosis experiments, untreated or S-layer-depleted *L. helveticus* MIMLh5 cells were fluorescently labelled using Alexa Fluor-conjugated succinimidyl-esters (SE-AF647; Alexa Fluor 647, Molecular Probes, Eugene, OR). Bacterial cells in Dulbecco's PBS (DPBS) were centrifuged for 5 min at 13,000 *g* in 1.5 ml Eppendorf tubes and resuspended in 750 µl of sodium carbonate buffer (pH 8.5); then SE-AF647 was added (10 µl for approximately 2×10^9 bacterial cells ml^{-1}). Bacteria were incubated at room temperature with agitation for 1 h in the dark, washed three times in sodium carbonate buffer, and finally resuspended in the original volume of DPBS.

Preparation of FITC-conjugated S-layer. The purified S-layer from *L. helveticus* MIMLh5 was dissolved in 5 M LiCl to obtain a 2 mg ml^{-1} protein solution, and the pH was adjusted to 9 by adding diluted NaOH. One ml of the protein solution was treated with 0.05 ml of a 1 mg ml^{-1} FITC solution in DMSO. The reaction was carried out overnight at 4 °C and stopped by adding 9 mL of 5 M urea in water. The FITC-conjugated protein solution was concentrated to 1 ml – while exchanging buffer to 5 M urea – by using an Amicon® Ultra-15 centrifugal filter unit (MWCO 10 kDa, Merck Millipore Ltd., Cork, Ireland). The FITC-labeled protein was stored at 4 °C.

S-layer adsorption on polystyrene nanoparticles (NPs). Fifty micrograms of Nile Red fluorescent (RF) polystyrene particles (NP) with an average size of 0.84 µm (Kisker Biotech, Steinfurt, Germany) were added to 1 ml of a 0.2 mg ml^{-1} FITC-labeled S-layer solution in 5M urea, and gently stirred at 4 °C for 2 hours. Then, the NP suspension was slowly diluted to a final volume of 10 ml by progressive addition of water over a several hours. The preparation was kept overnight at 4 °C under

stirring, and centrifuged at 10000 *g* for 30 m at 4 °C. The precipitated NPs were washed tree times with 5 M urea to remove unbound proteins, and the S-layer-coated NPs were suspended in 1 ml of ultrapure water.

Evaluation of *L. helveticus* MIMLh5 and S-layer-coated beads (Sl-beads) uptake by DCs. Non-adherent immature DCs were harvested and resuspended in complete medium to a concentration of 2×10^6 cells ml^{-1}. Pretreatment of cells with cytochalasin D (Sigma-Aldrich) at a final concentration of 0.5 µg ml^{-1} was performed in flasks for 1 h at 37 °C and 5% CO_2 in a humidified atmosphere before the addition of stimuli. After that, 150 µl of DCs were seeded (3×10^5 cells $well^{-1}$) in 96-well U-bottom tissue culture plates (NUNC) and incubated for 30 min at 37 °C and 5% CO_2 in a humidified atmosphere with either fluorescent beads (uncoated or S-layer coated), or with fluorescently labelled *L. helveticus* MIMLh5 (with and without a S-layer protein coating). Bacteria were used at a MOI of 5, and beads were tested at both MOI 5 and 50. All conditions were tested in triplicate, in at least three different experiments. Before each experiment, beads were treated in an ultrasound bath for at least 2 min to gently ensure size uniformity. All the stimuli were tested in absence and presence of cytochalasin D. Controls included untreated cells and cells incubated only with cytochalasin D without any stimulus. After incubation with beads and bacteria, DCs were spun down (1200 *g* × 5 min at 4 °C), washed twice with cold PBS containing 1% FCS (washing buffer), and then fixed with 1% formaldehyde in washing buffer. Cells were analyzed by flow cytometry on a FacsCantoII (BD Biosciences). Unless otherwise stated, data are from at least three independent experiments. Data analysis was performed using the FLOWJO version 10 software (Ashland, OR).

Statistical analysis. Statistical calculations were performed using the software program GraphPad Prism 5. The significance of the results was analyzed by unpaired heteroscedastic Student's t test with two-tailed distribution. Differences of $P < 0.05$ were considered significant.

Ethics statement. All animals used as a source of bone marrow cells were housed under conditions approved by the Danish Animal Experiments Inspectorate (Forsøgdyrstilsynet), Ministry of Justice, Denmark, and experiments were carried out in accordance with the guidelines 'The

Council of Europe Convention European Treaty Series 123 for the Protection of Vertebrate Animals used for Experimental and other Scientific Purposes'. Since the animals were employed as sources of cells, and no live animals were used in experiments, no specific approval was required for this study. Hence, the animals used for this study are included in the general facility approval for the faculty of Health and Medical Sciences, University of Copenhagen.

RESULTS

Depletion of S-layer from *L. helveticus* MIMLh5 reduces INF-β, IL-12 and IL-10 production by DCs. To study the role of S-layer protein in the *L. helveticus* MIMLh5-mediated induction of a Th1 activating response in DCs, we compared the levels of different cytokines produced by DCs upon stimulation with *L. helveticus* MIMLh5 or n-MIMLh5. SDS-PAGE confirmed that the protein was efficiently removed from bacterial surface, as evidenced by the strong reduction of the 45 kDa band corresponding to MIMLh5 S-layer protein, while leaving apparently unaltered the other proteins (**Fig. 1,** lanes 4-6). Then, the expression of *Ifnβ, Il12*, *Il10*, *Tnfα* and *Il1β* genes in DCs at 2, 4, 6 and 10 h was analyzed by RT-qPCR following stimulation with bacteria and the S-layer protein; furthermore, the concentrations of the corresponding cytokines was assessed by ELISA in DC supernatant collected after 10 h of incubation.

Removal of S-layer protein from the surface of MIMLh5 influenced the ability of the bacterium to induce *Ifnβ, Il12*, Il10, *Tnfa* and *Il1β* (**Fig. 2A**). ELISA data evidenced that the levels of IFN-β, IL12 and IL10 were significantly lowered in the supernatant of DCs stimulated with n-MIMLh5 compared to intact MIMLh5 (**Fig. 2B**). The purified S-layer protein did not induce the expression of *Ifnβ* or *Il12* at any of the considered time points (**Fig. 2A**), as also confirmed at protein level by ELISA at 10 h (**Fig. 2B).** In contrast, S-layer protein induced the expression of *Il10* and the pro-inflammatory cytokines *Tnfα* and *Il1β* (**Fig. 2A**), as also confirmed by corresponding cytokine quantification in DCs supernatant (**Fig. 2B**). Overall, n-MIMLh5 induced the same cytokine expression profile as MIMLh5, but to a lower extent (**Fig. 2A**). The cytokine concentrations in the

supernatant harvested after 10 h reflected the expression profiles of each gene, with a significant difference between n-MIMLh5 and MIMLh5 regarding IFN-β, IL-12 and IL-10 concentration (**Fig. 2B**).

The effect of MAPK-inhibition on IL-12 production does not differ between MIMLh5 and n-MIMLh5. To test whether *L. helveticus* MIMLh5 S-layer protein influences the signaling pathways that initiate IL-12 production by DCs, we investigated the effect of inhibiting specific mediators of the Mitogen Activated Protein (MAP) kinase cascade (Kaji et al., 2010), namely, JNK1/2, p38, and ERK 1/2. These pathways have previously been shown to be involved in *L. acidophilus* NCFM-dependent induction of IL-12 production in DCs (Weiss et al., 2011, 2012). The production of IL-12 was quantified by ELISA upon addition of MAPK inhibitors before bacterial stimulation. JNK1/2 inhibition resulted in a 26% and 39% reduction of IL-12 upon stimulation with *L. helveticus* MIMLh5 and n-MIMLh5, respectively (**Fig. 3**). Inhibition of p38 lowered IL-12 production by 24% (MIMLh5) and 66% (n-MIMLh5), whereas blocking ERK 1/2 caused an increase in IL-12 of 62% (MIMLh5) and 32% (n-MIMLh5) (**Fig. 3**).

Inhibition of bacterial endocytosis lowers IL-12 production in DCs stimulated with intact but not S-layer-depleted MIMLh5 cells. To test whether the S-layer protein affects endocytosis of *L. helveticus* MIMLh5 by DCs, we quantified IL-12, IL-10 and TNF-α by ELISA after stimulation of DCs with either MIMLh5 or n-MIMLh5 in the presence of cytochalasin D, an inhibitor of actin-dependent cytoskeleton rearrangement (Cooper, 1987). We found that the presence of cytochalasin D significantly lowered IL-12 production (by 27%) when DCs were stimulated with MIMLh5, whereas it did not significantly affect the IL-12 levels when DCs were stimulated with n-MIMLh5 (**Fig. 4A**). In addition, pre-treatment with cytochalasin D increased IL-10 production induced by MIMLh5 and n-MIMLh5 (**Fig. 4B**), whereas TNF-α levels were not significantly affected (**Fig. 4C**).

Endocytosis of *L. helveticus* MIMLh5 is partly dependent on the presence of S-layer protein on the bacterial surface. To study the endocytosis of *L. helveticus* MIMLh5 in DCs, we

prepared Alexa-Fluor 647-labelled cells of MIMLh5 and n-MIMLh5. Labeling was not equally efficient for the two bacteria and flow cytometry data thus not directly comparable. When DCs were pre-treated with cytochalasin D before addition of both bacterial preparations, we observed a major reduction in the number of fluorescent DCs (*i.e.* DCs that internalized fluorescence-labeled bacteria); nonetheless, the difference in the number of DCs positive for endocytosed bacteria between cytochalasin D-treated and untreated DCs was greater for the intact MIMLh5 than for n-MIMLh5, indicating a more pronounced endocytosis of MIMLh5 (**Fig. 5**).

To directly demonstrate the role of the S-layer in endocytosis, we coated fluorescent beads of a size resembling bacterial cells dimension (~ 800 nm) with the isolated MIMLh5 S-layer protein (Sl-beads). The quantity of beads employed to prepare Sl-beads to be used in comparative/chasing experiments was estimated on the basis of the bead average mass and of the volume of individual beads. In these experiments, we decided to use the beads at the same MOIs used for bacterial cells (5 and 50), even though it was not possible to assume that the amounts of S-layer protein on beads and bacterial surface were comparable. The presence of the S-layer protein with the fluorescent beads was demonstrated by SDS-PAGE (**Fig. 6A**, lanes 2-5), which shows bands at around 45 kDa. The slightly higher apparent size of proteins detached from Sl-beads (**Fig. 6A**, lanes 6-9) may relate to the extensive unfolding associated with non-covalent interaction of proteins with polystyrene nanoparticles (Barbiroli et al., 2015; Miriani et al., 2014).

Sl-beads and plain beads (*i.e.* fluorescence-labelled beads without any protein coating) were added to DCs, and the proportion of cells taking up beads was evaluated by flow cytometry (DCs positive of endocytosed beads; **Fig. 6B)**. When DCs were incubated with plain beads at MOI 50, about 28% of them endocytosed the beads, and addition of cytochalasin D only marginally reduced this number (from 28% to 22%; **Fig. 6B, C**), indicating that the majority of the beads were stuck on the DCs surface. Conversely, incubation with Sl-beads at MOI 50 gave a higher percentage of positive DCs compared to incubation with plain beads (53% positive), an effect that was also evident at MOI 5 (13% positive DCs in presence of Sl-beads vs 5% in presence of plain fluorescent

beads; **Fig. 6 B, D**). The addition of cytochalasin D prior to the addition of Sl-beads reduced the proportion of positive DCs from 13 to 8% at MOI 5, and from 53 to 35% with MOI 50 (**Fig. 6B, C, D**), indicating decreased internalization of coated beads compared to the plain ones.

DISCUSSION

Here we have demonstrated that depletion of S-layer from *L. helveticus* MIMLh5 significantly reduced the bacteria's capability to induce IFN-β, IL-12 and IL-10 in bone marrow derived dendritic cells. By contrast, no major reduction in the innate pro-inflammatory cytokines TNF-α and IL-1β was seen. S-layer, as isolated molecule, was a poor immune stimulator, only inducing a weak expression of the cytokines IL-10, TNF-α and IL-1β, and was unable to activate the expression of IFN-β and IL-12, even if we calculated that the amount of purified S-layer used was approximately 100 times more than the S-layer present on the bacterial surface of the amount of cells used in the same experiment. As we have previously demonstrated that induction of INF-β by lactobacilli only takes place in endosomes upon endocytosis of the intact bacteria (Weiss et al., 2010a, 2011), we hypothesized that S-layer plays a key role in the endocytosis of the bacteria. We have previously observed that lactobacilli can induce IL-12 by at least two distinct signaling pathways. One depends on the induction of IFN-β through a MAPK pathway inducing c-jun/ATF2 activation of AP-1, which is fully dependent on the MAPK JNK1/2 and, to much lesser degree on p38, while the MAPK ERK does not seem to be involved (Weiss et al., 2010b, 2011). The other pathway leads to direct induction of IL-12 and seems to depend on p38 (Lu et al. 1999; Weiss et al., 2011). Accordingly, we investigated how MAPK inhibitors of JNK1/2, p38 and ERK1/2 (*via* MEK) affected the IL-12 response upon stimulation with MIMLh5 or n-MIMLh5. The two bacterial stimulations demonstrated comparable effects as for sensitivity to JNK1/2 inhibition. By contrast, inhibition of p38 resulted in a marked IL-12 decrease after n-MIMLh5 stimulation, whereas the highest sensitivity to IL-12 inhibition by ERK1/2 was observed after stimulation with native, untreated MIMLh5. This let us to conclude that the S-layer depletion from MIMLh5 lowers its

ability to promote IFN-β-mediated IL-12 production. We hypothesized that this may be due to impaired endocytosis of the S-layer-depleted bacteria. This is supported by experiments with cytochalasin D-treated DCs that are unable to endocytose bacteria: the response induced by MIMLh5 was significantly reduced by cytochalasin D pre-treatment at contrast to n-MIMLh5. Likewise, we found a higher β-actin-dependent uptake of fluorescence-labelled MIMLh5 than of fluorescence-labelled n-MIMLh5. As we have previously demonstrated that another S-layer coated bacterium, *L. acidophilus* NCFM, is endocytosed partly by phagocytosis and partly by macropinocytosis in murine DCs (Boye et al., 2016), the difference between MIMLh5 and n-MIMLh5 in the endocytosis by DCs in presence of cytochalasin D may indicate that the S-layer-depleted bacteria are restricted in uptake by one of these mechanisms, most probably by phagocytosis. A comparison of the cytochalasin D effects on endocytosis and IL-12 production indicates that only some of the produced IL-12 is dependent on endocytosis of the bacteria. Along the same lines, the decrease of INF-β in DCs stimulated with S-layer-depleted MIMLh5 was not complete, which may indicate that some bacteria are still endocytosed by the constitutive micropinocytosis, that takes place independently from the cell wall structures present on the bacterial cells. To this end, we have previously shown that only a proportion of endocytosed *L. acidophilus* NCFM is taken up by phagocytosis while the rest was taken up by macropinocytosis (Boye et al., 2016; Fuglsang et al., 2017). The relative relevance of each event will depend on the properties of the bacteria, and most notably on the bacterial surface, as well as on ceramide formation on plasma membrane of DCs (Boye et al., 2016; Fuglsang et al, 2017; Abdel Shakor et al., 2004).

We tried to coat fluorescent beads of a size comparable to bacteria with the isolated S-layer protein, in order to investigate whether this would facilitate endocytosis of the beads. We found a significantly higher number of bead-positive DCs when S-layer-coated beads were added, compared to the addition of plain fluorescent beads. This supports a role of the S-layer in facilitating endocytosis. The naked beads are readily dispersed in water solutions with medium ionic strength

but at physiological p*I*, as used for this study, they may show some tendency to aggregate. Association with S-layer proteins are likely to change this property towards more readily dispersed particles at the physiologic ionic strength. From this study, we cannot establish whether the higher uptake of S-layer-associated beads is due to the binding to a specific receptor, to a stronger non-specific attraction to the negatively charged cell surface, or to a higher dispensability. However, held together with the results from studying the effect of the S-layer-depleted MIMLh5, these data support a role of S-layer in the endocytosis of MIMLh5. In summary, we have provided evidence that the S-layer of *L. helveticus* MIMLh5 is involved in endocytosis of the bacterium which is of importance for a strong Th1-inducing cytokine production. Moreover, this kind of knowledge can be of help in the selection of probiotic strains for specific purposes, e. g. in cases of exacerbated IgE production, allergies, and atopy where favoring a Th1 response would be of benefit.

COMPLIANCE WITH ETHICAL STANDARDS

Conflict of interest

The authors declare that they have no conflict of interest.

ACKNOWLEDGMENTS

We thank Anni Mehlsen, Matteo Miriani for precious technical assistance. This study was partially funded by the University of Milan Funding "Linea 2-2014", MAGIC-MAMPS.

REFERENCES

Fagan RP, Fairweather NF. 2014. Biogenesis and functions of bacterial S-layers. Nat Rev Microbiol. **12**:211-222.

Abdel Shakor AB, Kwiatkowska K, Sobota A. 2004. Cell surface ceramide generation precedes and controls FcgammaRII clustering and phosphorylation in rafts. J Biol Chem. **279**:36778-3687.

Barbiroli A, Bonomi F, Iametti S, Marengo M. 2015. Stabilization of the 'open' conformer of apoIscU on the surface of polystyrene nanobeads accelerates assembly of a 2Fe2S structure. Peptidomics **2**: 40-44.

Blaser, M. J. & Pei, Z. 1993. Pathogenesis of *Campylobacter fetus* infections: critical role of high-molecular-weight S-layer proteins in virulence. J. Infect. Dis. **167**:372–377.

Boye L, Welsby I, Lund LD, Goriely S, Frøkiaer H. 2016. Plasma membrane Toll-like receptor activation increases bacterial uptake but abrogates endosomal *Lactobacillus acidophilus* induction of interferon-β. Immunology. **149**:329-342.

Christensen HR, Frokiaer H, Pestka JJ. 2002. Lactobacilli differentially modulate expression of cytokines and maturation surface markers in murine dendritic cells. J Immunol **168**:171–178.

Cooper JA. 1987. Effects of cytochalasin and phalloidin on actin. J Cell Biol. **105**:1473-1478.

de Leeuw E, Li X, Lu W. 2006. Binding characteristics of the *Lactobacillus brevis* ATCC 8287 surface layer to extracellular matrix proteins. FEMS Microbiol Lett. **260**:210–215.

Doig P, Emödy L, Trust T.J. 1992. Binding of laminin and fibronectin by the trypsin-resistant major structural domain of the crystalline virulence surface array protein of *Aeromonas salmonicida*. J. Biol. Chem. **267**:43-49.

Fuglsang E, Boye L, Frøkiær H. 2017. Enhancement of ceramide formation increases endocytosis of *Lactobacillus acidophilus* and leads to increased IFN-β and IL-12 production in dendritic cells. J Clin Immunol Res. **1**:1-9.

Garcia-Vallejo JJ, van Kooyk Y. 2013. The physiological role of DC-SIGN: a tale of mice and men. Trends Immunol. **34**:482-486.

Granucci F, Petralia F, Urbano M, Citterio S, Di Tota F, Santambrogio L, Ricciardi-Castagnoli P. 2003. The scavenger receptor MARCO mediates cytoskeleton rearrangements in dendritic cells and microglia. Blood. **102**:2940-2947.

406 **Guglielmetti S, Taverniti V, Minuzzo M, Arioli S, Stuknyte M, Karp M, Mora D**. 2010a. Oral
407 bacteria as potential probiotics for the pharyngeal mucosa. Appl Environ Microbiol. 76:3948-
408 3958.
409 **Guglielmetti S, Taverniti V, Minuzzo M, Arioli S, Zanoni I, Stuknyte M, Granucci F, Karp M,**
410 **Mora D**. 2010b. A dairy bacterium displays in vitro probiotic properties for the pharyngeal
411 mucosa by antagonizing group A streptococci and modulating the immune response. Infect
412 Immun. 78:4734-4743.
413 **Hynönen U, Palva A.** 2013. *Lactobacillus* surface layer proteins: structure, function and
414 applications. Appl Microbiol Biotechnol. **97**:5225-5243.
415 **Kaji R, Kiyoshima-Shibata J, Nagaoka M, Nanno M, Shida K**. 2010. Bacterial teichoic acids
416 reverse predominant IL-12 production induced by certain lactobacillus strains into predominant
417 IL-10 production via TLR2-dependent ERK activation in macrophages. J Immunol. **184**:3505-
418 3513.
419 **Konstantinov SR, Smidt H, de Vos WM, Bruijns SC, Singh SK, Valence F, Molle D, Lortal S,**
420 **Altermann E, Klaenhammer TR, van Kooyk Y**. 2008. S layer protein A of *Lactobacillus*
421 *acidophilus* NCFM regulates immature dendritic cell and T cell functions. Proc Natl Acad Sci
422 USA. **105**:19474- 19479.
423 **Li P, Yu Q, Ye X, Wang Z, Yang Q**. 2011. *Lactobacillus* S-layer protein inhibition of *Salmonella*-
424 induced reorganization of the cytoskeleton and activation of MAPK signalling pathways in
425 Caco-2 cells. Microbiology. **157**:2639-2646.
426 **Liu Z, Roche PA**. 2015. Macropinocytosis in phagocytes: regulation of MHC class-II-restricted
427 antigen presentation in dendritic cells. Front Physiol. **6**:1-6.
428 **Livak, KJ, Schmittgen TD**. 2001. Analysis of relative gene expression data using real-time
429 quantitative PCR and the 2(-Delta Delta C(T)) method. Methods **25**: 402–408.
430 Miriani M, Iametti S, Kurtz DM, Bonomi F (2014) Rubredoxin refolding on nanostructured
431 hydrophobic surfaces: Evidence for a new type of biomimetic chaperones. Proteins 82: 3154–3162.

Powlesland AS, Ward EM, Sadhu SK, Guo Y, Taylor ME, Drickamer K 2006. Widely divergent biochemical properties of the complete set of mouse DC-SIGN-related proteins. J Biol Chem. **281**:20440- 20449.

Relloso M, Puig-Kröger A, Pello OM, Rodríguez-Fernández JL, de la Rosa G, Longo N, Navarro J, Muñoz-Fernández MA, Sánchez-Mateos P, Corbí AL. 2002. DC-SIGN (CD209) expression is IL-4 dependent and is negatively regulated by IFN, TGF-beta, and anti-inflammatory agents. J Immunol. 168:2634-2643.

Savina A, Amigorena S. 2007. Phagocytosis and antigen presentation in dendritic cells. Immunol Rev. **219**:143-156.

Smit E, Oling F, Demel R, Martinez B, Pouwels PH. 2001.The S-layer protein of *Lactobacillus acidophilus* ATCC 4356: identification and characterisation of domains responsible for S-protein assembly and cell wall binding. J Mol Biol. **305**:245-257.

Sun Z, Kong J, Hu S, Kong W, Lu W, Liu W. 2012. Characterization of a S-layer protein from *Lactobacillus crispatus* K313 and the domains responsible for binding to cell wall and adherence to collagen. Appl Microbiol Biotechnol. **97**:1941-1952.

Taverniti V, Dalla Via A, Minuzzo M, Del Bo' C, Riso P, Frøkiær H, Guglielmetti S. 2017. In vitro assessment of the ability of probiotics, blueberry and food carbohydrates to prevent *S. pyogenes* adhesion on pharyngeal epithelium and modulate immune responses. Food Funct. **8**:3601-3609.

Taverniti V, Stuknyte M, Minuzzo M, Arioli S, De Noni I, Scabiosi C, Cordova ZM, Junttila I, Hämäläinen S, Turpeinen H, Mora D, Karp M, Pesu M, Guglielmetti S. 2013. S-layer protein mediates the stimulatory effect of *Lactobacillus helveticus* MIMLh5 on innate immunity. Appl Environ Microbiol. **79**:1221-1231.

Taverniti V, Guglielmetti S. 2012. Health-Promoting Properties of *Lactobacillus helveticus*. Front Microbiol. **3**:392.

Taverniti V, Minuzzo M, Arioli S, Junttila I, Hämäläinen S, Turpeinen H, Mora D, Karp M, Pesu M, Guglielmetti S. 2012. In vitro functional and immunomodulatory properties of the *Lactobacillus helveticus* MIMLh5-*Streptococcus salivarius* ST3 association that are relevant to the development of a pharyngeal probiotic product. Appl Environ Microbiol. **78**:4209-4216.

Taverniti V, Guglielmetti S. 2011.The immunomodulatory properties of probiotic microorganisms beyond their viability (ghost probiotics: proposal of paraprobiotic concept). Genes Nutr. **6**:261-274.

Thompson SA. 2002. *Campylobacter* surface-layers (S-layers) and immune evasion. Ann. Periodontol. **7**:43-53.

Wang D, Sun B, Feng M, Feng H, Gong W, Liu Q, Ge S. 2015. Role of scavenger receptors in dendritic cell function. Hum Immunol. **76**:442-446.

Weiss G, Forster S, Irving A, Tate M, Ferrero RL, Hertzog P, Frøkiær H, Kaparakis-Liaskos M. 2013. *Helicobacter pylori* VacA suppresses *Lactobacillus acidophilus*-induced interferon beta signaling in macrophages via alterations in the endocytic pathway. MBio. **4**:e00609-12.

Weiss G, Maaetoft-Udsen K, Stifter SA, Hertzog P, Goriely S, Thomsen AR, Paludan SR, Frøkiær H. 2012. MyD88 drives the IFN-β response to *Lactobacillus acidophilus* in dendritic cells through a mechanism involving IRF1, IRF3, and IRF7. J Immunol. **189**:2860-2868.

Weiss G, Christensen HR, Zeuthen LH, Vogensen FK, Jakobsen M, Frøkiær H. 2011. Lactobacilli and bifidobacteria induce differential interferon-β profiles in dendritic cells. Cytokine. **56**:520-530.

Weiss G, Rasmussen S, Zeuthen LH, Nielsen BN, Jarmer H, Jespersen L, Frøkiaer H. 2010a. *Lactobacillus acidophilus* induces virus immune defence genes in murine dendritic cells by a Toll-like receptor-2-dependent mechanism. Immunology. **131**:268-281.

Weiss G, Rasmussen S, Nielsen Fink L, Jarmer H, Nøhr Nielsen B, Frøkiaer H. 2010b. *Bifidobacterium bifidum* actively changes the gene expression profile induced by *Lactobacillus acidophilus* in murine dendritic cells. PLoS One. **5**:e11065.

Zeuthen LH, Fink LN, Frøkiaer H. 2008. Toll-like receptor 2 and nucleotide-binding oligomerization domain-2 play divergent roles in the recognition of gut-derived lactobacilli and bifidobacteria in dendritic cells. Immunology. **124**:489-502.

Zhu C, Guo G, Ma Q, Zhang F, Ma F, Liu J, Xiao D, Yang X, Sun M. 2017. Diversity in S-layers. Prog Biophys Mol Biol. **123**:1-15.

LEGENDS

Fig. 1. SDS-PAGE profile of crude cell extract obtained by boiling *L. helveticus* MIMLh5 cells before and after LiCl treatment. M, molecular weight marker. Lanes 1-3, extracts from 2.5×10^8, 3.75×10^8 and 5×10^8 intact MIMLh5 cells, respectively; lanes 4-6, extracts from 2.5×10^8, 3.75×10^8 and 5×10^8 LiCl-treated MIMLh5 cells, respectively.

Fig. 2. Cytokine profile elicited in bone marrow-derived dendritic cells (DCs) by *L. helveticus* MIMLh5 cells with and without (n-MIMLh5) S-layer and by purified S-layer protein. Expression of cytokines *Ifn*β, *Il12*, *Il10*, *Tnf*α and *Il1*β was determined by RT-qPCR after 2, 4, 6 and 10 h incubation (A). Expression profiles are indicated as the fold change of induction (FOI) relative to the control (unstimulated DCs) which was set at a value of 1 (A). Asterisks indicate statistically significant differences between MIMLh5 and nMIMLh5 (**: $P < 0.01$; *: $P < 0.05$) according to two-way ANOVA analysis along the time-course experiment (A). Protein levels of IFN-β, IL-12, IL-10, TNF-α and IL-1β were measured in the supernatants of DCs by ELISA after 10 h of incubation (B). Slay: S-layer protein from *L. helveticus* MIMLh5 was used at a concentration of 10 μg ml^{-1}. MIMLh5 cells and S-layer depleted MIMLh5 cells (n-MIMLh5) were both used at a multiplicity of infection (MOI) of 50. C: unstimulated DCs. Data represent mean of measurements from triplicates ± standard deviation. Asterisks indicate statistically significant differences between MIMLh5 and n-MIMLh5 (*: $P < 0.05$) according to unpaired t-test.

Fig. 3. Stimulation of DCs with *L. helveticus* MIMLh5, S-layer-depleted MIMLh5 cells (n-MIMLh5), and the purified S-layer protein after pre-incubation with inhibitors for JNK 1/2, p38 and MEK 1/2. Protein levels of the cytokines IL-12 were measured in the supernatants of DCs by ELISA after 20 h. MIMLh5 and n-MIMLh5 were used at a MOI of 50. Slay: S-layer protein was tested at a concentration of 10 μg ml^{-1}. C: control (unstimulated DCs). MAPK inhib: DCs stimulated only with respective MAPK inhibitors JNK, p38 and MEK. Asterisks indicate statistically significant differences (***: $P < 0.001$; **: $P < 0.01$) according to unpaired t-test. Data represent mean of measurements from triplicate cultures ± standard deviation.

Fig. 4. Cytokine production in DCs upon stimulation with *L. helveticus* MIMLh5 and S-layer-depleted MIMLh5 (n-MIMLh5) in presence of cytochalasin D. DCs were prestimulated for 1 h with cytochalasin D (0.5 μg ml^{-1}) before addition of bacterial cells. Protein levels of the cytokines IL-12 (A), IL-10 (B) and TNF-α (C) were measured in the supernatants of DCs by ELISA after 20 h. MIMLh5 LiCl-treated and untreated cells were used at a MOI of 5. N-MIMLh5: MIMLh5 cells after removal of the S-layer protein by LiCl-extraction. C: control (unstimulated DCs). Cyt D: DCs stimulated only with the cytochalasin D. Asterisks indicate statistically significant differences (**: $P < 0.01$; *: $P < 0.05$) according to unpaired t-test. Data represent mean of measurements from triplicate cultures ± standard deviation.

Fig. 5. DCs were pretreated with cytochalasin D or media (no bacteria) for 1 h before stimulation with Alexa Fluor 647-labelled *L. helveticus* MIMLh5 for 30 min followed by flow cytometry analysis. Data in the histograms (A) are reported as fold of decrease of the number of DCs positive for endocytosed MIMLh5 and upon treatment with cytochalasin D compared to the untreated DCs. Fluorescent untreated MIMLh5 (B) and n-MIMLh5 cells (C) were used at a MOI of 5. n-MIMLh5: MIMLh5 cells after removal of the S-layer protein by LiCl-extraction. APC positive population: DCs uptaking bacteria (B, C). Asterisks indicate statistically significant differences (***: $P < 0.001$) according to unpaired t-test. Dot plots are based on 50.000 cells counted on FACS CantoII and single cell gating by the use of FSC-A/FSC-H. Means and SD are based on technical replicates.

Fig. 6. The presence of S-layer protein from MIMLh5 on polystyrene beads preparation, revealed by SDS-PAGE with Coomassie blue staining, affects endocytosis in DCs. In lanes 2 to 5 of the SDS-gel the following estimated MOIs of S-layer-coated beads (Sl-beads) were loaded: 20-30-40-50. In lanes 6 to 9 the following quantity of S-layer protein have been loaded: 5-10-15-20 μg. (A). DCs were pretreated with cytochalasin D or media (no beads) for 1 h before stimulation with fluorescent beads prolonged for 1 h, followed by flow cytometry analysis (B, C, D). The percentage of DCs that have endocytosed beads by macropinocytosis is indicated as percentage of DCs positive

of endocytosed beads (B). Fluorescent plain beads (B, C) and fluorescent beads coated with FITC-S-layer protein (Sl-beads) (B, D) were used at a corresponding MOI of 5 and 50. PE positive population: DCs uptaking beads (C, D). Asterisks indicate statistically significant differences (***: $P < 0.001$; *: $P < 0.05$) according to unpaired t-test. Dot plots are based on 50.000 cells counted on FACS CantoII and single cell gating by the use of FSC-A/FSC-H. Means and SD are based on technical replicates.

Fig. 1

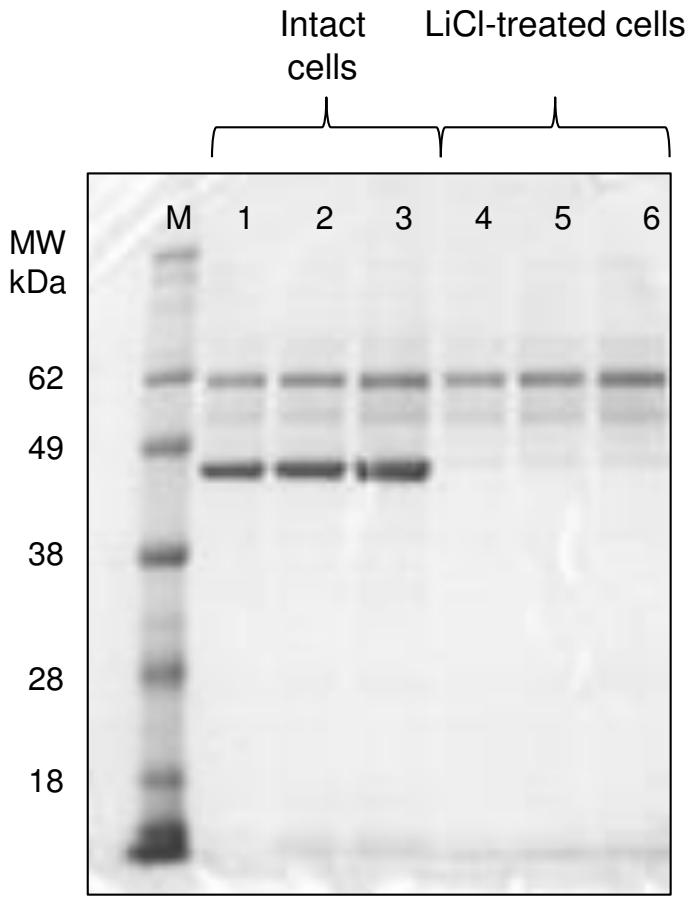

Fig. 2

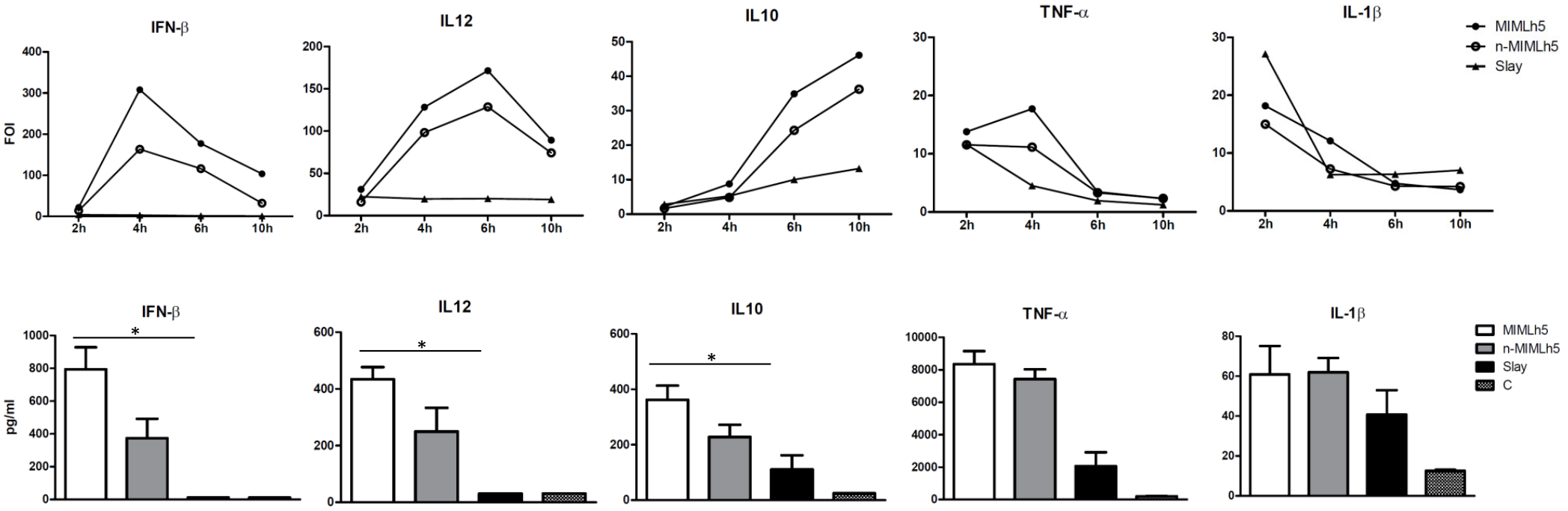
IFN-β
IL12
IL10
TNF-α
IL-1β
FOI
2h
4h
6h
10h
MIMLh5
n-MIMLh5
Slay
pg/ml
*
C

Fig. 3

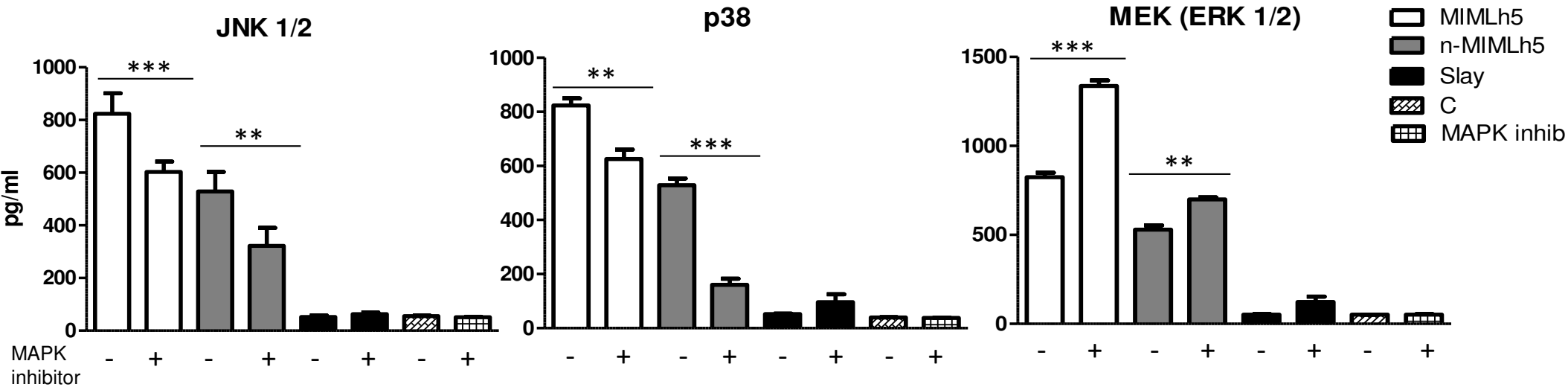
JNK 1/2
p38
MEK (ERK 1/2)
MIMLh5
n-MIMLh5
Slay
C
MAPK inhib
pg/ml
1000
800
600
400
200
0
1500
1000
500
***
**
***
**
***
**
MAPK
inhibitor
- + - + - + - +

Fig. 4

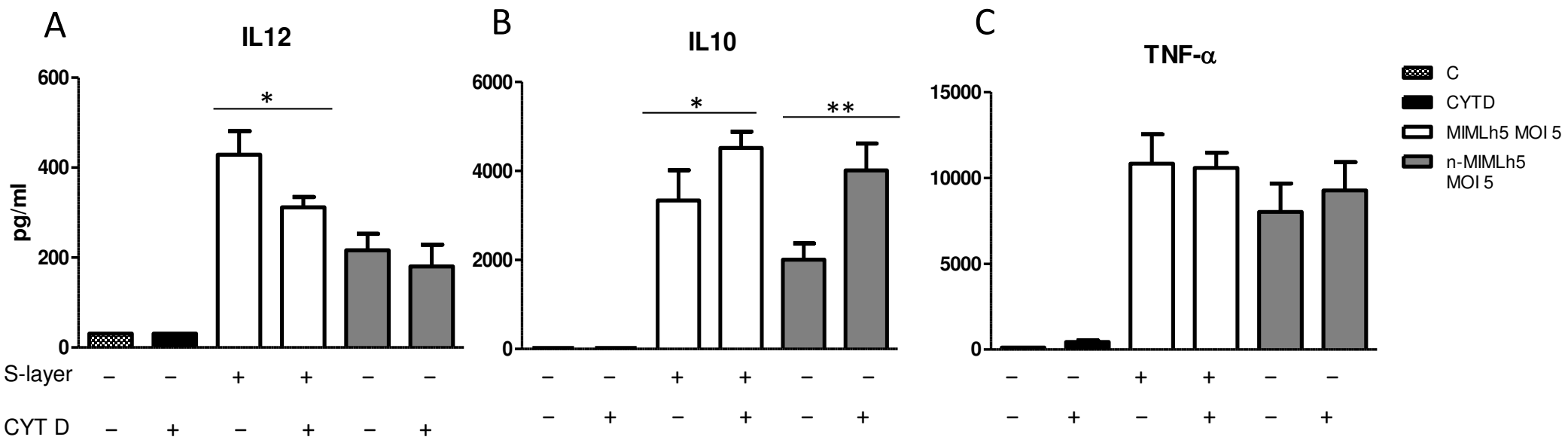
A
IL12
600
400
200
0
pg/ml
*
B
IL10
6000
4000
2000
0
*
**
C
TNF-α
15000
10000
5000
0
C
CYTD
MIMLh5 MOI 5
n-MIMLh5 MOI 5
S-layer
CYT D

Fig. 5

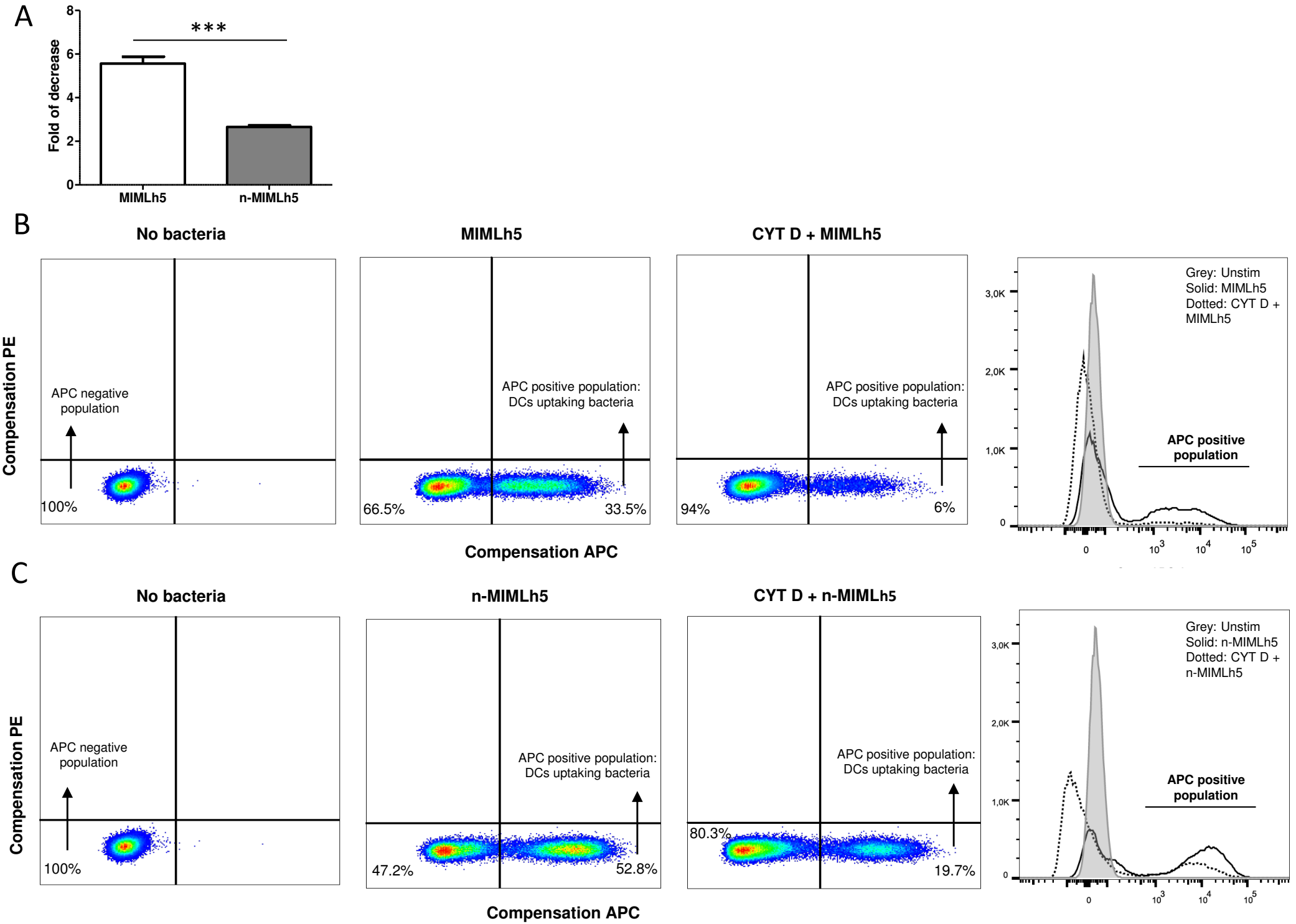
A
***
Fold of decrease
8
6
4
2
0
MIMLh5
n-MIMLh5
B
No bacteria
MIMLh5
CYT D + MIMLh5
Compensation PE
APC negative population
100%
APC positive population: DCs uptaking bacteria
66.5%
33.5%
APC positive population: DCs uptaking bacteria
94%
6%
Grey: Unstim
Solid: MIMLh5
Dotted: CYT D + MIMLh5
APC positive population
3,0K
2,0K
1,0K
0
Compensation APC
C
No bacteria
n-MIMLh5
CYT D + n-MIMLh5
Compensation PE
APC negative population
100%
APC positive population: DCs uptaking bacteria
47.2%
52.8%
APC positive population: DCs uptaking bacteria
80.3%
19.7%
Grey: Unstim
Solid: n-MIMLh5
Dotted: CYT D + n-MIMLh5
APC positive population
3,0K
2,0K
1,0K
0
Compensation APC

Fig. 6

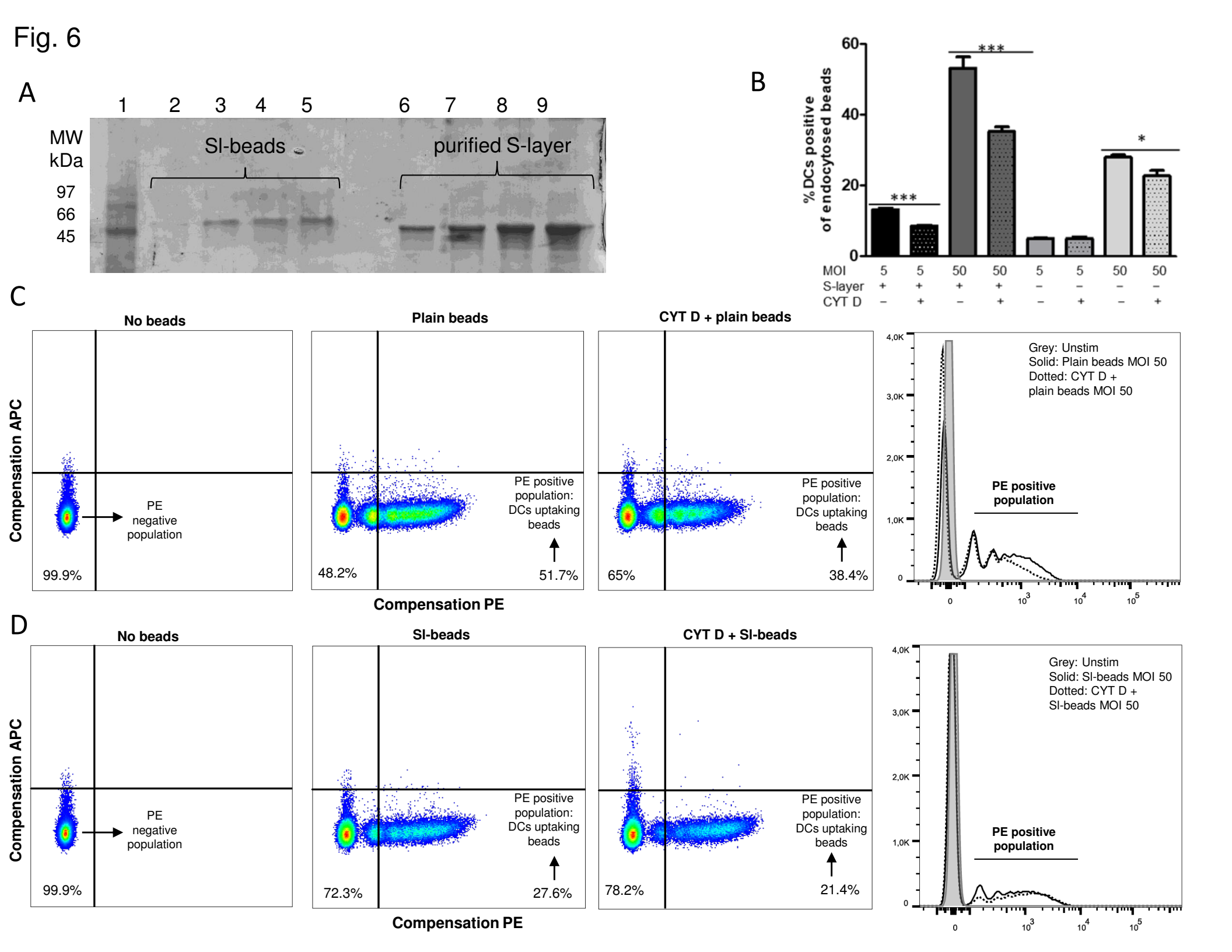
A
1 2 3 4 5 6 7 8 9
MW kDa
97
66
45
Sl-beads
purified S-layer
B
% DCs positive of endocytosed beads
60
40
20
0
***
***
*
MOI 5 5 50 50 5 5 50 50
S-layer + + + + – – – –
CYT D – + – + – + – +
C
No beads
Plain beads
CYT D + plain beads
Compensation APC
PE negative population
99.9%
PE positive population: DCs uptaking beads
48.2%
51.7%
65%
38.4%
Compensation PE
Grey: Unstim
Solid: Plain beads MOI 50
Dotted: CYT D + plain beads MOI 50
PE positive population
4,0K
3,0K
2,0K
1,0K
0
10^3
10^4
10^5
D
No beads
Sl-beads
CYT D + Sl-beads
Compensation APC
PE negative population
99.9%
PE positive population: DCs uptaking beads
72.3%
27.6%
78.2%
21.4%
Compensation PE
Grey: Unstim
Solid: Sl-beads MOI 50
Dotted: CYT D + Sl-beads MOI 50
PE positive population